

**COMPARATIVE PERFORMANCE OF ALOS PALSAR  
POLARIZATION BANDS AND ITS COMBINATION  
WITH ALOS AVNIR-2 DATA FOR LAND COVER  
CLASSIFICATION**

**SIM CHONG KEAT**

**UNIVERSITI SAINS MALAYSIA**

**2012**

## ACKNOWLEDGEMENT

First of all I would like to express my sincere thank and gratitude to my main supervisor, Assoc. Prof. Khiruddin Abdullah, who had been spending times and efforts on supervising me throughout the research. The dedicated guidance, inspiration, comments, suggestions, and advice provided are greatly appreciated. Without the patience, care and concern from Assoc. Prof. Khiruddin Abdullah, this project will not be completed steadily. Again, hearty thanks to Assoc. Prof. Khiruddin Abdullah for being a great supervisor.

I am particularly grateful to my co-supervisor Prof. Mohd. Zubir Mat Jafri for his help, support and sharing of information and thought throughout this project. I wish to express my sincere appreciation to Assoc. Prof. Lim Hwee San for the problem solving in data analysis, time, and also the help in reviewing the paper written for peer reviewing journals from the study.

Moreover, the helps and technical supports from the staff of School of Physics, namely Mr. Azmi Abdullah, Mr. Burhanuddin Wahi from Engineering Physics Laboratory, Mr Shahil Ahmad Khosani, Mr. Mydin Jamal and Mr. Yaakub Othman from Geophysics Laboratory are greatly appreciated.

Besides, I would like to acknowledge Japan Aerospace Exploration Agency (JAXA) for providing free ALOS PALSAR and ALOS AVNIR-2 data. My appreciation goes to ASF Map Ready for Alaska satellite Facility Geographical Institute at the University of Alaska Fairbanks for providing ASF MapReady programs free software for public access.

Furthermore, I would like to convey a million of thanks to all my lab mates from Engineering Physics Laboratory, who never fails in supporting, encouraging and stand by me through the thick and thin.

Not forgetting Universtiti Sains Malaysia, for rewarding me USM fellowship which covers my tuition fee and living expenses during the research and Postgraduate Research Grant Scheme (USM-RU-PRGS) (Grant No. 1001/PFIZIK/832005) which helped to carry out this project.

Last but not least, the constant and invaluable supports, loves, care and concerns from my dearest parents, my sisters, and my bother are highly appreciated. Without their help and encouragement, I would unable to complete this study.

## TABLE OF CONTENTS

	Page
ACKNOWLEDGEMENTS	ii
TABLE OF CONTENTS	iv
LIST OF TABLES	viii
LIST OF FIGURES	x
LIST OF ABBREVIATION	xii
ABSTRAK	xv
ABSTRACT	xvii
<b>CHAPTER 1- INTRODUCTION</b>	
1.0 Introduction	1
1.1 Problem Statement	4
1.2 Scope of the study	5
1.3 Research Objectives	5
1.4 Novelty of this study	6
1.5 Structure of the Thesis	6
<b>CHAPTER 2- LITERATURE REVIEWS</b>	
2.0 Introduction	7
2.1 Literature Reviews	7
2.2 Satellite Data	13
2.2.1 ALOS	13
2.2.1.1 ALOS PALSAR	14
2.2.1.2 ALOS AVNIR-2	15
2.2.2 ASTER GDEM	16
2.3 Summary	18
<b>CHAPTER 3- STUDY AREA,RESEARCH MATERIAL AND METHODOLOGY</b>	
3.1 Overview of Study Area	19
3.1.1 Penang	19
3.1.2 Perak	22
3.1.3 Kedah	23
3.2 Processing Software	23
3.2.1 ASF MapReady 2.3	24
3.2.2 PCI Geomatica 10.3	24
3.2.3 Garmin E-Trex Vista Hcx	25
3.3 Methodology	26
3.3.1 Data Acquisition	26
3.3.1.1 Original Radar	26
3.3.1.2 ALOS AVNIR-2	27
3.3.1.3 ASTER DEM	28
3.3.1.4 Ground Truth	29
3.3.2 Workflow	30
3.3.3 Images Pre-processing	32
3.3.3.1 ALOS PALSAR	32
3.3.3.2 ALOS AVNIR-2	33
3.3.3.3 Geometric Correction	33

3.3.3.4	Subset of study Area	35
3.3.3.5	Overlay of ALOS PALSAR and ALOS AVNIR-2 data	35
3.4	Data Processing and Analysis	35
3.4.1	Transform Divergence	35
3.4.2	Speckle Filtering	36
3.4.2.1	Enhanced Frost Filter (EF)	37
3.4.2.2	Enhanced Lee Filter (EL)	37
3.4.2.3	Lee Filter (L)	37
3.4.2.4	Frost Filter (F)	37
3.4.2.5	Gamma Map Filter (GM)	38
3.4.2.6	Kuan Filter (K)	38
3.4.3	Texture Analysis	39
3.4.4	Principal Component Analysis (PCA)	41
3.4.5	Image Combination	42
3.5	Classification	43
3.5.1	Supervised classification	44
3.5.2	Training Area Selection	45
3.6	Accuracy Assessments	45
3.7	Summary	47
<b>CHAPTER 4- RESULTS AND DISCUSSION</b>		
4.0	Introduction	48
4.1	Geometric Correction	48
4.2	Penang	48
4.2.1	Original Radar	49
4.2.1.1	Transformed Divergence	51
4.2.1.2	Radar classification	53
4.2.2	Radar Filtered	58
4.2.2.1	Enhanced Frost, Enhanced Lee, Lee, Kuan, and Gamma Filter	58
4.2.2.2	Frost Filter	58
4.2.2.3	Radar Filtered Classification	61
4.2.3	Radar Texture	64
4.2.3.1	Median, Variance, Skewness, Mean Euclidean Distance, and Kurtosis	65
4.2.3.2	Mean	65
4.2.3.3	Radar Texture Classification	67
4.2.4	Radar Combination: Radar filtered with radar texture	71
4.2.5	Sensor Combination	72
4.2.5.1	Layer stacking	73
4.2.5.2	Principal Component Analysis (PCA)	76
4.3	Perak	81
4.3.1	Original Radar	81
4.3.1.1	Transformed Divergence	83
4.3.1.2	Radar classification	84
4.3.2	Radar Filtered	88
4.3.2.1	Enhanced Frost, Enhanced Lee, Lee, Kuan, and Gamma Filter	89

4.3.2.2	Frost Filter	89
4.3.2.3	Radar Filtered Classification	91
4.3.3	Radar Texture	94
4.3.3.1	Median, Variance, Skewness, Mean Euclidean Distance, and Kurtosis	95
4.3.3.2	Mean	95
4.3.3.3	Radar Texture Classification	96
4.3.4	Radar Combination: Radar filtered with radar texture	99
4.3.5	Sensor Combination	101
4.3.5.1	Layer stacking	102
4.3.5.2	Principal Component Analysis (PCA)	105
4.4	Kedah	109
4.4.1	Original Radar	109
4.4.1.1	Transformed Divergence	111
4.4.1.2	Radar classification	112
4.4.2	Radar Filtered	116
4.4.2.1	Enhanced Frost, Enhanced Lee, Lee, Kuan, and Gamma Filter	117
4.4.2.2	Frost Filter	117
4.4.2.3	Radar Filtered Classification	119
4.4.3	Radar Texture	122
4.4.3.1	Median, Variance, Skewness, Mean Euclidean Distance, and Kurtosis	123
4.4.3.2	Mean	123
4.4.3.3	Radar Texture Classification	125
4.4.4	Radar Combination: Radar filtered with radar texture	128
4.4.5	Sensor Combination	131
4.4.5.1	Layer stacking	131
4.4.5.2	Principal Component Analysis (PCA)	134
4.5	Summary	137
<b>CHAPTER 5- CONCLUSION AND FUTURE WORKS</b>		
5.0	Introduction	139
5.1	Conclusions	139
5.2	Suggestions for Future Research	142
<b>REFERENCES</b>		143
<b>APPENDICES</b>		
Appendix 1:	ALOS PALSAR image acquisition date	151
Appendix 2:	ALOS AVNIR-2 image acquisition date	151
Appendix 3:	Ground control points coordinate taken while doing ground truth in Penang, Perak and Kedah.	151
	Table A: Ground Control Points Coordinate for Penang	151
	Table B: Ground Control Points Coordinate for Perak	152
	Table C: Ground Control Points Coordinate for Kedah	152
Appendix 4:	Class separability values from original radar for polarization, Penang	153
Appendix 5:	TD values for the remaining filter with different filter size, Penang	153

<b>Appendix 6: TD values for frost filter with different filter size, Penang</b>	<b>154</b>
<b>Appendix 7: TD values for the remaining texture with different window size, Penang.</b>	<b>157</b>
<b>Appendix 8: TD values for mean texture, Penang</b>	<b>157</b>
<b>Appendix 9: Class separability values from original radar for polarization, Perak</b>	<b>160</b>
<b>Appendix 10: TD values for the remaining filter with different filter size, Perak</b>	<b>161</b>
<b>Appendix 11: TD values for frost filter with different filter size, Perak</b>	<b>162</b>
<b>Appendix 12: TD values for the remaining texture with different window size, Perak</b>	<b>163</b>
<b>Appendix 13: TD values for mean texture, Perak</b>	<b>164</b>
<b>Appendix 14: Class separability values from original radar for polarization, Kedah</b>	<b>165</b>
<b>Appendix 15: TD values for the remaining filter with different filter size, Kedah</b>	<b>166</b>
<b>Appendix 16: TD values for frost filter with different filter size, Kedah</b>	<b>167</b>
<b>Appendix 17: TD values for the remaining texture with different window size, Kedah</b>	<b>169</b>
<b>Appendix 18: TD values for mean texture, Kedah</b>	<b>169</b>
<b>LIST OF PUBLICATIONS</b>	<b>172</b>

## LIST OF TABLES

	<b>Page</b>
<b>Table 2.1</b> PALSAR Major Characteristics	15
<b>Table 2.2</b> AVNIR-2 Major Characteristics	16
<b>Table 2.3</b> ASTER bands with resolution of 30 meters	17
<b>Table 3.1</b> The specification of GPS	25
<b>Table 4.1</b> RMS Result of the study areas	48
<b>Table 4.2</b> Backscattering coefficients from original radar, Penang	49
<b>Table 4.3</b> Classification accuracies for original radar images, Penang	53
<b>Table 4.4</b> TD values for frost filter with different filter size, Penang	59
<b>Table 4.5</b> Classification accuracies for Frost filtered images, Penang	61
<b>Table 4.6</b> TD values for mean texture, Penang	66
<b>Table 4.7</b> Classification accuracies for the Mean Texture 11 x 11 images, Penang	68
<b>Table 4.8</b> Classification accuracies for filtered radar with radar texture, Penang	71
<b>Table 4.9</b> Classification accuracies filtered radar with ALOS AVNIR-2, Penang	73
<b>Table 4.10</b> Classification accuracies radar texture with ALOS AVNIR-2, Penang	75
<b>Table 4.11</b> PCA of Filtered Radar with PCA ALOS AVNIR-2, Penang	77
<b>Table 4.12</b> PCA of Radar texture with ALOS AVNIR-2, Penang	79
<b>Table 4.13</b> Backscattering coefficients from original radar, Perak	81
<b>Table 4.14</b> Classification accuracies for original radar images,Perak	85
<b>Table 4.15</b> TD values for frost filter with different filter size, Perak	89
<b>Table 4.16</b> Classification accuracies for Frost filtered images, Perak	91
<b>Table 4.17</b> TD values for mean texture, Perak	95



<b>Table 4.18</b>	Classification accuracies for the Mean Texture 11 x 11 images, Perak	97
<b>Table 4.19</b>	Classification accuracies for filtered radar with radar texture, Perak	100
<b>Table 4.20</b>	Classification accuracies filtered radar with ALOS AVNIR-2, Perak	102
<b>Table 4.21</b>	Classification accuracies radar texture with ALOS AVNIR-2, Perak	104
<b>Table 4.22</b>	PCA of Filtered Radar with PCA ALOS AVNIR-2, Perak	106
<b>Table 4.23</b>	PCA of Radar texture with PCA ALOS AVNIR-2, Perak	107
<b>Table 4.24</b>	Backscattering coefficients from original radar, Kedah	109
<b>Table 4.25</b>	Classification accuracies for original radar images, Kedah	113
<b>Table 4.26</b>	TD values for frost filter with different filter size, Kedah	117
<b>Table 4.27</b>	Classification accuracies for Frost filtered images, Kedah	119
<b>Table 4.28</b>	TD values for mean texture, Kedah	123
<b>Table 4.29</b>	Classification accuracies for the Mean Texture 11 x 11 images, Kedah	125
<b>Table 4.30</b>	Classification accuracies for filtered radar with radar texture, Kedah	129
<b>Table 4.31</b>	Classification accuracies filtered radar with ALOS AVNIR-2, Kedah	131
<b>Table 4.32</b>	Classification accuracies radar texture with ALOS AVNIR-2, Kedah	133
<b>Table 4.33</b>	PCA of Filtered Radar with PCA ALOS AVNIR-2, Kedah	134
<b>Table 4.34</b>	PCA of Radar texture with PCA ALOS AVNIR-2, Kedah	136

## LIST OF FIGURES

	Page
<b>Figure 1.1</b> The Electromagnetic Spectrum (EMS) (CRISP,2011)	2
<b>Figure 2.1</b> ALOS satellite	14
<b>Figure 3.1</b> Location of the study area	21
<b>Figure 3.2</b> Original radar image of the study areas	27
<b>Figure 3.3</b> True colors of ALOS AVNIR-2 Satellite images	28
<b>Figure 3.4</b> DEM images of the study areas	29
<b>Figure 3.5</b> Overview of workflow methodology	31
<b>Figure 3.6</b> The Process of Geometric Correction (PCI,2003)	34
<b>Figure 4.1</b> The polarizations of L-band between different kinds of land cover classes	50
<b>Figure 4.2</b> TD values between different polarizations of L-band, Penang	52
<b>Figure 4.3</b> Producer's Accuracy using MLC classifier with different combination of original radar data, Penang	55
<b>Figure 4.4</b> User's Accuracy using MLC classifier with different combination of original radar data, Penang	56
<b>Figure 4.5</b> Classified map of the original data, Penang	57
<b>Figure 4.6</b> Producer's Accuracy using MLC classifier with different combination of Frost filtered data, Penang	62
<b>Figure 4.7</b> User's Accuracy using MLC classifier with different combination of Frost filtered data, Penang	63
<b>Figure 4.8</b> Classified map of Frost filtered data, Penang	64
<b>Figure 4.9</b> Producer's Accuracy using MLC classifier with different combination of mean texture data, Penang	69
<b>Figure 4.10</b> User's Accuracy using MLC classifier with different combination of mean texture data, Penang	69
<b>Figure 4.11</b> Classified map of mean texture data, Penang	70
<b>Figure 4.12</b> Classified map of radar filter with radar texture data, Penang	72

<b>Figure 4.13</b>	Classified map of filtered radar with ALOS AVNIR-2 data, Penang	74
<b>Figure 4.14</b>	Classified map of radar texture with ALOS AVNIR-2, Penang	76
<b>Figure 4.15</b>	Classified map of PCA of filtered radar with PCA of ALOS AVNIR-2 data, Penang	78
<b>Figure 4.16</b>	Classified map of PCA of radar texture with PCA of ALOS AVNIR-2 data, Penang	80
<b>Figure 4.17</b>	Polarizations of L-band between different land cover classes, Perak	82
<b>Figure 4.18</b>	TD values between different polarizations of L-band, Perak	83
<b>Figure 4.19</b>	Producer's Accuracy using MLC classifier with different combination of original radar data, Perak	86
<b>Figure 4.20</b>	User's Accuracy using MLC classifier with different combination of original radar data, Perak	87
<b>Figure 4.21</b>	Classified map of the original data, Perak	88
<b>Figure 4.22</b>	Producer's Accuracy using MLC classifier with different combination of Frost filtered data, Perak	93
<b>Figure 4.23</b>	User's Accuracy using MLC classifier with different combination of Frost filtered data, Perak	93
<b>Figure 4.24</b>	Classified map of Frost filtered data, Perak	94
<b>Figure 4.25</b>	Producer's Accuracy using MLC classifier with different combination of Mean texture data, Perak	98
<b>Figure 4.26</b>	User's Accuracy using MLC classifier with different combination of Mean texture data, Perak	98
<b>Figure 4.27</b>	Classified map of mean texture data, Perak	99
<b>Figure 4.28</b>	Classified map of radar filter with radar texture data, Perak	101
<b>Figure 4.29</b>	Classified map of filtered radar with ALOS AVNIR-2 data, Perak	103
<b>Figure 4.30</b>	Classified map of radar texture with ALOS AVNIR-2, Perak	105
<b>Figure 4.31</b>	Classified map of PCA of filtered radar with PCA of ALOS AVNIR-2 data, Perak	106
<b>Figure 4.32</b>	Classified map of PCA of radar texture with PCA of ALOS AVNIR-2 data, Perak	108

<b>Figure 4.33</b>	Polarizations of L-band between different land cover classes, Kedah	110
<b>Figure 4.34</b>	TD values between different polarizations of L-band, Kedah	112
<b>Figure 4.35</b>	Producer's Accuracy using MLC classifier with different combination of original radar data, Kedah	114
<b>Figure 4.36</b>	User's Accuracy using MLC classifier with different combination of Original radar data, Kedah	115
<b>Figure 4.37</b>	Classified map of the original data, Kedah	116
<b>Figure 4.38</b>	Producer's Accuracy using MLC classifier with different combination of Frost filtered data, Kedah	120
<b>Figure 4.39</b>	User's Accuracy using MLC classifier with different combination of Frost filtered data, Kedah	121
<b>Figure 4.40</b>	Classified map of Frost filtered data, Kedah	122
<b>Figure 4.41</b>	Producer's Accuracy using MLC classifier with different combination of Mean texture data, Kedah	126
<b>Figure 4.42</b>	User's Accuracy using MLC classifier with different combination of Mean texture data, Kedah	127
<b>Figure 4.43</b>	Classified map of mean texture data, Kedah	128
<b>Figure 4.44</b>	Classified map of radar filter with radar texture data, Kedah	130
<b>Figure 4.45</b>	Classified map of filtered radar with ALOS AVNIR-2 data, Kedah	132
<b>Figure 4.46</b>	Classified map of radar texture with ALOS AVNIR-2, Kedah	133
<b>Figure 4.47</b>	Classified map of PCA of filtered radar with PCA of ALOS AVNIR-2 data, Kedah	135
<b>Figure 4.48</b>	Classified map of PCA of radar texture with PCA of ALOS AVNIR-2 data, Kedah	137

## LIST OF ABBREVIATION

ALOS	Advanced Land Observation Satellite
ANN	Artificial Neural Network
ASF	Alaska satellite Facility
ASTER	Advanced Spaceborne Thermal Emission and Reflection Radiometer
Avg	Average
AVNIR-2	Advanced Visible and Near Infrared Radiometer type 2
B	Blue
DN	Digital Number
EF	Enhanced Frost Filter
EL	Enhanced Lee Filter
EMS	Electromagnetic Spectrum
EOS	Earth Observing System
ERSDAC	Japan's Earth Remote Sensing Data Analysis Centre
F	Frost Filter
G	Green
GCPs	Ground Control Points
GM	Gamma Map Filter
GPS	Global Positioning System
IHS	Intensity Hue Saturation
IR	Infrared
JAXA	Japan Aerospace Exploration Agency
K	Kuan Filter
KNN	K Nearest Neighbor
KU	Kurtosis
L	Lee Filter
M	Mean
MAP	Maximum A Posteriori
MED	Mean Euclidian Distance
METI	Japan's Ministry of Economy, Trade and Industry
ML	Maximum Likelihood
MLC	Maximum Likelihood Classifier
MN	Median
NASA	National Aeronautics and Space Administration
NIR	Near Infrared
PA	Producer's Accuracy
PALSAR	Phased Array type L-band Synthetic Aperture Radar
PCA	Principal Component Analysis
PLR	Polarimetric
PRISM	Panchromatic Remote-sensing Instrument for Stereo Mapping
R	Red
RBF	Radial Basis Function
RMS	Root Mean Square
ROIs	Region of Interests
S	Skewness
SAR	Synthetic Aperture Radar
SLC	Single Look Complex
SVM	Support Vector Machine

TD	Transform Divergence
UA	User's Accuracy
UTM	Universal Transverse Mercator
UV	Ultraviolet
V	Variance
WIST	Warehouse Inventory Search Tool
WML	Wishart Maximum Likelihood
2D	Two-dimensional

# **PRESTASI KOMPARATIF BAGI JALUR-JALUR PENGKUTUBAN ALOS PALSAR DAN GABUNGANNYA DENGAN ALOS AVNIR-2 DATA UNTUK PENGELASAN LITUPAN TANAH**

## **ABSTRAK**

Data penderiaan jauh gelombang mikro telah digunakan secara meluas untuk pengelasan litupan tanah di persekitaran kita. Dalam kajian ini, jalur-jalur pengkutuban ALOS PALSAR digunakan untuk mengenalpasti ciri-ciri litupan tanah bagi tiga kawasan kajian di Malaysia. Kawasan kajian tersebut terdiri daripada kawasan terpilih dari Pulau Pinang, Perak dan Kedah. Tujuan kajian ini adalah untuk mengkaji prestasi data ALOS PALSAR yang dinilai secara bebas dan gabungan data ini dengan ALOS AVNIR-2 untuk pengelasan litupan tanah.

Program ASF MapReady dari Alaska satellite Facility Geographical Institute di University of Alaska Fairbanks telah digunakan untuk pra-pemprosesan data ALOS PALSAR. Di samping itu, pelbagai teknik pemprosesan imej yang berlainan termasuk penurasan bintik, pengukuran tekstur dan Analisis Komponen Utama (PCA) telah diaplikasikan pada data ALOS PALSAR. Kaedah pengelasan terselia Maximum Likelihood Classifier (MLC) telah digunakan untuk imej ALOS PALSAR dalam analisis pengelasan litupan tanah. Pelbagai kelas litupan tanah telah dikenal pasti dan dinilai dengan menggunakan pengukuran pengasingan perubahan kecapahan (TD). Kawasan latihan data PALSAR telah dipilih berdasarkan maklumat yang diperolehi dari data ALOS AVNIR-2.

Data asal memberikan hasil yang kurang memuaskan dalam mengenal pasti kelas litupan tanah kerana kehadiran bintik yang banyak. Penurasan Frost secara

signifikan telah memperbaiki ketepatan pengelasan namun masih belum memadai untuk pengelasan litupan tanah yang tepat. Pengekstrakan dan penggunaan pengukuran tekstur min didapati sangat bermanfaat apabila menilai pengasingan di antara litupan tanah yang berbeza. Oleh itu, tekstur min mampu menyediakan ketepatan pengelasan yang lebih tinggi berbanding dengan data asal radar dan data penurasan radar. Gabungan data ALOS PALSAR dengan ALOS AVNIR-2 memberi ketepatan pengelasan yang terbaik. Ketepatan keseluruhan tertinggi telah dicapai melalui gabungan min tekstur radar dengan ALOS AVNIR-2 data. Kajian ini membuktikan bahawa litupan tanah di Pulau Pinang, Perak dan Kedah boleh dipetakan secara tepat dengan menggunakan gabungan data optik dan radar.



**COMPARATIVE PERFORMANCE OF ALOS PALSAR POLARIZATION  
BANDS AND ITS COMBINATION WITH ALOS AVNIR-2 DATA FOR  
LAND COVER CLASSIFICATION**

**ABSTRACT**

Microwave Remote Sensing data have been widely used for land cover classification in our environment. In this study, ALOS PALSAR polarization bands were used to identify land cover features in three study areas in Malaysia. The study area consists of Penang, Perak and Kedah. The aims of this research are to investigate the performance of ALOS PALSAR datasets which are assessed independently and combination of these data with ALOS AVNIR-2 for land cover classification.

ASF MapReady program from Alaska satellite Facility Geographical Institute at the University of Alaska Fairbanks was used for the preprocessing of ALOS PALSAR data. In addition, different image processing techniques included Speckle Filtering, Texture measures, and Principal Component Analysis (PCA) were applied to the ALOS PALSAR datasets. Standard supervised classification method Maximum Likelihood Classifier (MLC) was applied to the ALOS PALSAR images for land cover classification analysis. Various land cover classes were identified and assessed using the Transformed Divergence (TD) separability measures. The PALSAR data training areas were chosen based on the information obtained from ALOS AVNIR-2 datasets.

The original data gave very poor results in identifying land cover classes due to the presence of immense speckle. Frost Filter significantly improved the

classification accuracies but still not adequate for accurate land cover classification. The extraction and use of mean texture measures was found to be very advantageous when evaluating the separability among the different land covers. Hence, mean texture was capable to provide higher classification accuracies as compared to the original radar and filtered radar data. Combination of ALOS PALSAR with ALOS AVNIR-2 consistently provided excellent classification accuracies. The highest overall accuracy was achieved by combining the radar mean texture with ALOS AVNIR-2 data. This study proved that the land cover of Penang, Perak, and Kedah can be mapped accurately using combination of optical and radar data.

# CHAPTER 1

## INTRODUCTION

### 1.0 Introduction

Remote sensing technology has been widely used for land cover application. It is important in many scientific and commercial application involving economic planning, resource management, environmental studies, restoration projects and disaster preparedness. The scientific analysis and interpretation of data has been enhanced using satellite-borne optical and radar sensors.

Over the past few decades, manual and computer-assisted image interpretation techniques were applied to optical Landsat MSS, Landsat TM, SPOT and ALOS imagery to classify land cover (Johnson and Rohde, 1981; Hutchinson, 1982; Tucker et al., 1985; Franklin et al., 1986; Gross et al., 1988). The manual interpretation was also aided with color infrared visual analysis. However, use of only optical imagery is unreliable under conditions of continued cloud cover that can persist over large areas of the earth's surface (Roebig et al., 1984).

In recent years, researchers have been investigating the use of longer wavelength radar imagery to obtain additional land cover information. The longer wavelengths of radar imagery is capable to produce images independently of sun illumination and weather conditions where traditional spaceborne optical and multispectral systems fails to provide timely and continuous information (Kasischke et al., 1997; Henderson et al., 2002). As shown in Figure 1, microwaves are longer than all other wavelengths with the exception of radio waves. These microwave

wavelengths hold enormous data collecting potential for many geographic areas around the world that are often obscured by cloud cover.

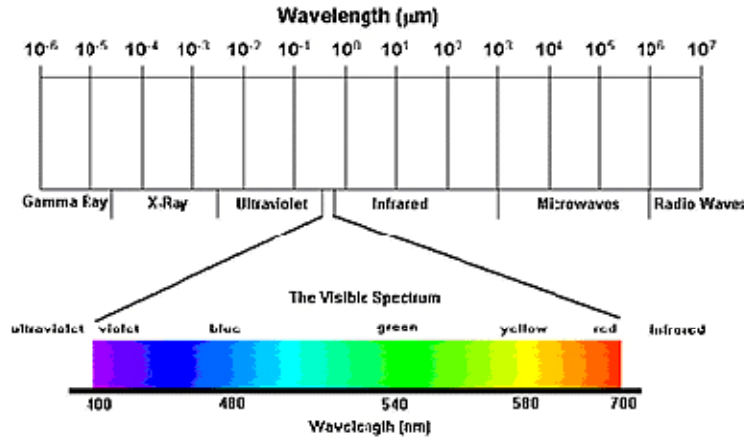


Figure 1.1 The Electromagnetic Spectrum (EMS). (CRISP, 2011)

Several single-frequency synthetic aperture radar (SAR) systems such as those aboard ERS-1 (C-band, VV polarization), RADARSAT (C-Band, HH polarization), and JERS-1 (L band, HH polarization) have been launched. The potential of SAR in land cover analysis has been clearly demonstrated (Dobson et al., 1995; Henderson and Lewis, 1998). Radar sensors are capable of precisely measuring the amount of returned energy, i.e., backscatter, and can accurately delineate the terrain regardless of the time and weather (Campbell, 2002). However, there are still many problems in radar data processing and applications such as radar speckle noise, banding noise, and fusion (Xie et al., 2004).

Most recent radar systems collecting data using single wavelength with a fixed polarization is a primary factor influencing the analysis of radar data. Hence only one component of the total surface scattering is being measured, while any additional information contained within the returned radar signal is lost (Toyra et al. 2001; Dell'Acqua et al. 2003). ALOS PALSAR and RADARSAT-2 increased

number of polarizations. Multiple polarization radar imagery will obtain different backscatter characteristics and different informational content (Banner and Ahern, 1995; Hegarat-Mascle et al. 1997; Gauthier et al. 1998).

The microwave energy transmitted and received by the radar can be horizontally or vertically polarized. In this way the electromagnetic field can be restricted to a vibration in the vertical or horizontal plane. A radar system can thus work in four different polarizations modes. A radar system can be HH, VV, VH or HV polarized. Like polarizations transmit and receive the same polarization and cross polarization, HV and VH are capable of transmitting and receiving polarizations which are orthogonal to each other (Campbell, 2002).

Land cover classification is one of the most frequently extracted information from remote sensing data. It represents a complex mixture of natural and anthropogenic ground classes (Kalensky, 1996). There are a number of radar image processing techniques and classification methods available at the moment, such as Transform Divergence (TD), adaptive speckle filtering, texture analysis, Maximum Likelihood Classification (MLC), Principle Component Analysis (PCA), and Fusion. But there are comparatively few studies concerned the comparative evaluation of the image processing techniques and the classification methods on the same data and even less studies have been done in land cover classification.

## **1.1 Problem Statement**

Maintaining up-to-date land-cover information can be very expensive and time consuming with the traditional methods of field and air photo interpretation. Nowadays, the development of remote sensing has become a cost efficient and effective alternative.

Unlike passive optical sensors which usually detect reflected solar radiation in the visible and infrared part of the electromagnetic spectrum, Synthetic Aperture Radar (SAR) is active sensor and works with microwave which could penetrate clouds, smog and haze, so SAR can image the Earth's surface day and night in almost all weathers. These properties make SAR systems an attractive data source for land-use/land-cover mapping, especially when optical data is not available due to various reasons.

Historically, most spaceborne radars were single wavelength and single polarization. For this study, the Japanese ALOS (Advanced Land Observing Satellite) PALSAR (Phased type L-band Synthetic Aperture Radar) quad polarization radar data seems to be most promising solution for land cover classification. Quad polarizations can be additional sensor parameter to detect specific object characteristic such as differences in plant structure, leaf roughness and leaf orientation, moisture content, soil roughness, harvesting effects, and land use pattern.

## **1.2 Scope of the Study**

This study examines the land cover classification over three study areas which include the selected areas of Penang, Perak and Kedah. For this study, the Japanese ALOS PALSAR quad polarization radar data were obtained at 12.5 meter spatial resolution. The second dataset to be used in this study was acquired by ALOS AVNIR-2 at a 10 meter spatial resolution. Several image processing methods have been carried out in this study are Transformed Divergence (TD), speckle filtering, texture measure analysis, principle component analysis (PCA), and layer stacking. Standard supervise classification technique Maximum Likelihood Classifier (MLC) was used for land cover classification. Finally, accuracy assessments and validation results were performed.

## **1.3 Research Objectives**

The objectives of this study are as follows:

1. To investigate the accuracy of each mode of quad polarization bands based on Transformed Divergence for each study areas.
2. To evaluate the effectiveness of different speckle filter and texture measures for image classification as compared to original radar images.
3. To assess overall classification accuracy by combining radar datasets and multi sensor combinations.

#### **1.4 Novelty of this study**

Studying the land cover classification by using the ALOS PALSAR quad polarization radar is new in Penang, Perak and Kedah. There are a number of radar image processing techniques and classification methods available at the moment, such as Transform Divergence (TD), speckle filtering, texture analysis, and Maximum Likelihood Classification (MLC). But there are comparatively few studies concerned the comparative evaluation of the radar image processing techniques on the same data, and even less studies have been done in Malaysia particularly the study area that include the selected areas of Penang, Perak and Kedah.

#### **1.5 Structure of the Thesis**

This thesis consists of five chapters. First chapter provides an overview of this study, problem statement, scope of the research, research objectives and novelty of this study. Literature reviews and satellite data has been used in this research are presented in chapter two. Chapter three describes the study areas, research materials and methodology that have been used for this research. Chapter four presents all the results for this research. This chapter also consist the discussion of the outcome of the processing analyses. Chapter five summarizes all the output and result for this research. Recommendations for future study are also included in this chapter.



## CHAPTER 2

### LITERATURE REVIEW

#### 2.0 Introduction

This chapter discusses studies about image processing method on land cover classification by other scientists, including their results and how their studies relate to this study.

#### 2.1 Literature Review

Remote Sensing is essentially the process of observing and collecting useful information for an object, area, or phenomenon without being in physical contact with that particular target (Siegal, 1980). Radar wavelength has a fundamental influence on the interaction between the electromagnetic wave and the natural medium (Garestier et al. 2006). The longer wavelengths have a higher penetration (Campbell, 2002). Thus different wavelength systems can be used for different aims. Dabrowska-Zielinska et al., (2007) highlighted C band is very suitable for crop monitoring, when the differences in phenological states between adjacent parcels can be directly observed. In the same way, long wavelengths are sometimes preferred for forest observation since major structuring elements can be detected while ignoring small leaves and branches. This is one of the established properties for radar systems: the longer the wavelength the larger the penetration (Mathieu, et al., 2003).

Polarization give advantages to radar images because polarization can be additional sensor parameter to detect specific object characteristic such as differences in plant structure, leaf roughness and leaf orientation, moisture content,

soil roughness, harvesting effects, land use pattern and etc (Buiten and Clevers, 1993). For generally speaking, large collection of structure with relatively little or no vegetation appear quite visible on HH polarization, but other areas such as residential or low density uses are less distinct (Ahmed, 2006). The HV polarization would be preferred in analyzing the other land uses within the urban area, while for VV polarization is the least desirable for urban landscape analysis (Evans et al., 1988)

The L band PALSAR images were effective to observation; high resolution, global coverage, and strategic data acquisition, enable us to identify land-cover characteristics and its changes (Masato et al. 2008). Schmidt (1986) found that airborne X-band radar was preferred for defining urban patterns while L-band was preferred in detecting individual buildings (Ban, and Wu, 2005). Besides, L bands have been consistently identified by several authors as the best frequencies for extraction of physical structural parameters of forest areas such as biomass and leaf area index (Richard et al. 1987; Quinones and Hoekman, 2004; Patenaude et al, 2005).

The polarization characteristics of electromagnetic energy recorded by a remote sensing system represent an important variable that can be used in many Earth resource investigations (Jensen, 2004). Multiple-polarized RADAR imagery is especially useful application of polarized energy (Jensen, 2004). Hussin (1995) studied the effect of polarization and incidence angle ( $28^{\circ}$ ,  $45^{\circ}$ , and  $58^{\circ}$ ) on radar return using L-band aircraft radar data and concluded that radar corner reflection from building is highly affected by the type of polarization and the degree of incidence angle. The dynamic range of the like-polarized component is larger than that of the cross-polarized component for urban areas; this is in contrast to the

measurement for forested areas, where the dynamic range of the cross-polarized component is larger than that of the like-polarized component (Dong et al. 1997).

Several studies demonstrated that multi-polarization SAR datasets have great potential for land cover classification (Saatchi and Rignot, 1997), forest mapping (Dobson et al., 1995), wetlands delineation (Proisy et al., 2002), agricultural applications (Karjalainen et al., 2008), and coastal mapping (Baghdadi et al., 2007). Davidson et al (2006) predict the single-look accuracy of various modes of ALOS PALSAR for a simple urban and vegetation discrimination problem. The use of additional polarizations may require additional time and operating power and it is important to justify this by increased classification accuracy (Davidson et al., 2006).

A Transformed Divergence (TD) separability measure is an indirect estimate of the likelihood of correct classification between different datasets or derived measures (Swain and Davis, 1978). A TD value of 1,500 or greater generally indicates an acceptable separability of classes (Latty and Hoffer, 1980). In previous studies undertaken by Haack (1984); Sheoran (2009), TD values provides a framework for selecting the best bands for land cover classification purposes. This separability technique were consistently used to not only evaluate separability, but also proved useful in eliminating many of the redundancies of multiple classifications.

The effect of speckle on the polarimetric parameter estimation was first investigated by Goodman in optics (1963; 1975; 1985). Speckle filtering of polarimetric SAR images as been an active area of research for a decade (Schou and Skriver, 2001). Tauzi and Lopes (1994) was the first to show that a conventional one-channel filter cannot preserve the polarimetric information and that speckle

filtering should be applied in terms of covariance matrices and not in terms of scattering matrices (Tauzi, 2002). Subsequently, various filters that provide filtered covariance matrices, or the equivalent filtered Mueller, Kennaugh, or target coherency matrix, have been developed (Tauzi, 2004). Speckle filter preserves the local information better and degrades less the geometrical resolution of the initial image (Desnos et al. 1993 and Lopes et al. 1993). Commonly used filters for reducing the high-frequency noise (speckle) while preserving the high-frequency features (edge) include Lee filter, Enhanced Lee filter, Frost filter, Enhanced Frost filter, Kuan filter and Gamma filter etc with different window sizes, iterations and other parameters (Shi & Fung 1994). Intensity-Driven Adaptive-Neighborhood Technique proposed by Vasile et al. (2006) is a relatively new spatial filter which is very effective. Adaptive filters have proven to be the most effective at distinguishing between useful information such as texture and speckle and are deemed to be most suitable for classification processes (Durand et al., 1987; Nyongui et al., 2002; Xiao et al., 2003).

The spatial and scale properties of texture in different surfaces such as rocks, sea-ice, seawater, vegetation, urban areas, etc. can be characterized by distinct textural features (Kandaswamy et al. 2005). For analysis of remotely sensed images, the GLCM-based methods are the most predominant (Baraldi & Parmiggiani 1995; Soh & Tsatsoulis 1999; Kandaswamy et al. 2005). The proper use of texture features could improve classification of SAR images (Paudyal et al. 1995). A large number of studies have been carried out to use texture information to improve the classification accuracy of SAR images (Dell'Acqua and Gamba, 2006, Dell'Acqua et al., 2003, Dekker 2003).

Traditionally, land cover classification has been done using optical images. In later year, the fusing data has been a common technique and this trend is bound to continue as the geospatial technologies improve greatly. The processing and fusing of such separate datasets, has made the synergies between optical and radar data for land applications of greater practical importance (Leckie, 1990; Pal et al. 2007). With its origin in military application, image combination has provided a framework for the civilian sector which helps integrate different sensor platforms for a variety of uses (Roberts et al. 2008).

Fusing data from multiple sensors, i.e., Landsat and radar has proved to be an exceptionally efficient technique in reducing the overall ambiguity in the datasets. Previous studies has been conducted by Sheoran et al. (2007), have suggested an increase in the overall classification values by fusing multiple datasets together. Chu and Ge (2010) have indicated that the combination of SAR data and optical images gives significantly higher classification accuracy than using a single type of data.

The joint processing of SAR and multispectral data increased the accuracies of biomass estimation and land use classifications. The efficiency of the method at medium spatial resolutions allows its application of global datasets (Lehman et al. 2011). The fusing of data from different sensors is done in an attempt to generate an interpretation of a geographic area that is not obtainable from any single sensor alone. This is also done to reduce the uncertainty associated with data from a single source (Schistad et al. 1994; Saraf, 1999; Simone et al. 2002).

There are distinct advantages of fusing radar with optical data, as the end product has the advantage of textural information (radar image), and spectral

information from the optical and infrared bands. Hence, by fusing multiple datasets, an analyst has a single and more informative image (Pal et al. 2007).

Idol et al (2008) was used Layer stacking as the primary method for combining different bands and datasets. In their analysis, layer stacking provided the platform for yielding good classification and separability results. A similarly techniques have been shown by Sheoran et al. (2007) which analysis of layer stacking was successfully in combination different datasets.

Principal Component Analysis (PCA) is an efficient method to summarize the most dominant spatial and spectral characteristic of the datasets (Henebry and Rieck, 1996). PCA has been successfully used in previous studies for land cover mapping and geological assessments (Pal et al, 2006, Chavez et al, 1991). Even though the use of PCA might result in good quality images, the limitations of this technique, as reported in many research papers were color distortion and loss of spectral information (Nikolakopoulos, 2008).

Classification techniques are widely used for land cover mapping and can be used as base information for many different applications. There are various techniques for classification such as Decision Tree Induction, Bayesian Classification, and Neural Networks (Han & Kamber, 2001). Sebastiano and Roli (1995) used K- nearest neighbor (KNN) along with other classifiers to classify the land-cover using multi sensor images.

A comparison between the Wishart Maximum Likelihood (WML) classifier with the recent NN-based classifier and evolutionary Radial Basis Function (RBF) classifier by Ince et al (2010) showed the effectiveness of the proposed algorithm. Wishart Maximum Likelihood (WML) method provides the highest accuracies in

both training and testing area in comparison between Neural Network (NN) classifier and evolutionary Radial Basis Function (RBF) methods. Sheoran et al. (2009) conducted the Maximum Likelihood classifier (MLC) analyses on three different study sites which include California, Kenya and Bangladesh. Lim et al, (2007a) proposed frequency based contextual classifier over Penang Island, Malaysia indicated the higher overall accuracy (>90%).The results from this multispectral classification analysis of the study area indicated that urban features could be clearly identified and classified relative to the surrounding terrain and its associated desert features.

Beh et al. (2010) carried out classification analysis on distribution of mangrove cover in Penang Island. High accuracy was obtained from the error matrix by using supervised maximum likelihood classification. Supervised classification of MLC was used in their research. The accuracy statistics was the measuring scale of the classification. MLC is the best classifier for the classification.

## **2.2 Satellite Data**

There are numerous satellites orbiting the Earth with different characteristics. The selection of data is dependent on the application, user's need and scale. This chapter describes the remote sensing system as well as data used in this research project.

### **2.2.1 ALOS**

The Advanced Land Observation Satellite (ALOS) was launched by Japan Aerospace Exploration Agency (JAXA) on January 24, 2006 (Figure 2.1). The satellite is placed in a sun synchronous orbit at 691 km. The orbital revisit period is

46 days, with a potential 2-day revisit capability for the side-looking instruments (Rosenqvist et al., 2004). Onboard, ALOS has three instruments; one Panchromatic Remote-sensing Instrument for Stereo Mapping (PRISM), one multispectral sensor Advanced Visible and Near Infrared Radiometer type 2 (AVNIR-2) and finally the Phased Array type L-band Synthetic Aperture Radar (PALSAR).

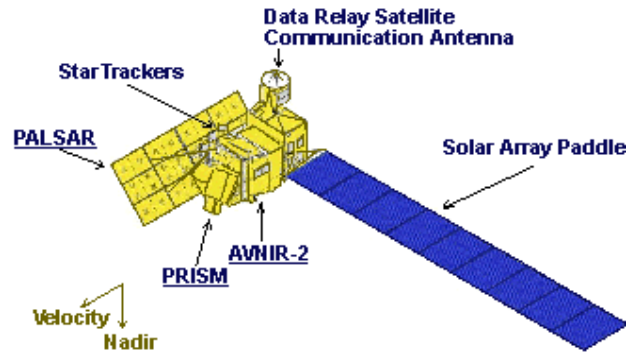


Figure 2.1 ALOS satellite

### 2.2.1.1 ALOS PALSAR

ALOS PALSAR is designed for acquisition of data beneficial to resources exploration, environmental protection and analysis. The sensor is a fully polarimetric instrument operating in either single polarization (HH or VV), dual polarization (HH, HV or VV, VH), or quad-polarization (HH, HV, VH, VV) mode. The look angle is variable between  $7^\circ$  and  $51^\circ$  ( $8-60^\circ$  incidence angles). The nominal ground resolution is  $\sim 10$  and  $\sim 20$  meters in the single- and dual-polarization modes, respectively, and  $\sim 30$  meters in quad-polarization mode. PALSAR can also operate in a coarse, 100 meter, resolution ScanSAR mode, with single polarization (HH or VV) and 250-350 km swath width (Rosenqvist et al., 2004). The specification of ALOS PALSAR is shown in Table 2.1.



Table 2.1 PALSAR Major Characteristics

<b>Mode</b>	<b>Fine Scan</b>		<b>Polarimetric</b>
<b>Center Frequency</b>	1270 MHz(L-band)		
<b>Chirp Bandwidth</b>	28MHz	14MHz	14MHz
<b>Polarization</b>	HH or VV	HH+HV or VV+VH	HH+HV+VH+VV
<b>Incident angle</b>	8 to 60 deg.	8 to 60 deg.	8 to 30 deg.
<b>Range Resolution</b>	7 to 44m	14 to 88m	24-89m
<b>Observation Swath</b>	40 to 70 km	40 to 70 km	20 to 65km
<b>Bit Length</b>	5 bits	5 bits	3 or 5bits
<b>Data rate</b>	240Mbps	240Mbps	240Mbps
<b>NE sigma zero *2</b>	< -23dB (Swath Width 70km)		< -29dB
	< -25dB (Swath Width 60km)		
<b>S/A *2,*3</b>	> 16dB (Swath Width 70km)		> 19dB
	> 21dB (Swath Width 60km)		
<b>Radiometric accuracy scene</b>	1dB / orbit: 1.5 dB		
<b>size of Antenna</b>	azimuth :8.9m x elevation :3.1m		

Source: (Advanced Land Observation Satellite / ALOS / Three Sensors for ALOS, 2011)

In addition, PALSAR systems operates in microwave regions, making it independent on sun illumination and weather conditions, it can capture images in descending and ascending mode day and night (De Grandi, et al., 1999). Thus, the polarimetric SAR is configured to record both the amplitude and phase of the backscattered signal for each of the four linear polarization configurations (HH, HV, VH and VV). The signals actually are recorded in complex notation from which their amplitude and phases could be computed (Ulaby et al., 1990; Richards et al., 1987).

### 2.2.1.2 ALOS AVNIR-2

The basic design concept of AVNIR-2 mission is the data continuity from ADEOS/AVNIR (Shimada et al., 1997).The difference from AVNIR is improvement of spatial resolution of multispectral (NIR, R, G, B) radiometer from 16m to 10m and the elimination of panchromatic mode because PRISM will undertake the high resolution panchromatic observation. The primary objectives of

AVNIR-2 are disaster monitoring and land cover mapping and with its across-track viewing capabilities (+/- 44°), observation of disaster areas within two days' repeat is feasible (Rosenqvist et al., 2004). The side-looking capacity also allows simultaneous observations with the PALSAR – a unique property and a “satellite first”. AVNIR-2 operates with a 120 Mbps data rate, which means that direct data downlink without the use of DRTS is possible (Rosenqvist et al., 2007). The specification is shown in Table 2.2.

Table 2.2 AVNIR-2 Major Characteristics

<b>Parameters</b>	<b>Information</b>
<b>Number of Bands</b>	4
<b>Wavelength</b>	Band 1 : 0.42 to 0.50 micrometers Band 2 : 0.52 to 0.60 micrometers Band 3 : 0.61 to 0.69 micrometers Band 4 : 0.76 to 0.89 micrometers
<b>Spatial Resolution</b>	10m (at Nadir)
<b>Swath Width</b>	70km (at Nadir)
<b>S/N</b>	>200
<b>MTF</b>	Band 1 through 3 : >0.25 Band 4 : >0.20
<b>Number of Detectors</b>	7000/band
<b>Pointing Angle</b>	- 44 to + 44 degree (Triplet Mode, Cross-track direction)
<b>Bit Length</b>	8 bits

Source: (Advanced Land Observation Satellite / ALOS / Three Sensors for ALOS, 2011)

## 2.2.2 Spaceborne Thermal Emission and Reflection Radiometer Global Digital

### Elevation (ASTER GDEM)

ASTER is an imaging instrument flying on Terra, a satellite launched in December 1999 as part of NASA's Earth Observing System (EOS). ASTER is a cooperative effort between NASA, Japan's Ministry of Economy, Trade and Industry (METI) and Japan's Earth Remote Sensing Data Analysis Centre (ERSDAC) (ASTER, 2011). However, the release of ASTER GDEM was only announced on June 29, 2009 by METI and NASA. The GDEM was created by stereo-correlating

the 1.3 million scene ASTER VNIR archive; it covers between 83°N and 83°S latitudes, or 99% of the earth’s surface, thereby making it the most complete mapping of the earth ever made. The GDEM has a resolution of 30 meters and is formatted in 1 x 1 degree tiles as GeoTIFF files. Each GDEM file is accompanied by a quality assessment file, either providing the number of ASTER scenes used to calculate a pixel’s value or indicating the source of the external DEM data used to fill the ASTER voids (NASA, 2011).

The goal of ASTER’s creation is to observe, understand, and model the earth’s weather system to discover how it is changing, better predict changes, and understand the consequences of these changes for life on Earth. ASTER is used to obtain detailed maps of land surface temperature, reflectance and elevation. ASTER provides high-resolution images of the earth in 15 different bands of the electromagnetic spectrum, ranging from visible to thermal infrared light. Although the resolution of ASTER images ranges between 15 and 90 metres, only the 30-metre resolution was used in this study, due to the certainty of its usage. Table 2.3 shows the ASTER 6 bands with a resolution of 30 metres used to produce the level 3 data product known as GDEM.

Table 2.3 ASTER GDEM bands with resolution of 30 meters

<b>Band No</b>	<b>Wavelength(μm)</b>	<b>Absolute Accuracy (σ)</b>	<b>Resolution (m)</b>	<b>Nadir</b>	<b>Description</b>
<b>4</b>	1.600–1.700	≤±4%	30	Nadir	Short-wave
<b>5</b>	2.145–2.185	≤±4%	30	Nadir	Infrared (SWIR)
<b>6</b>	2.185–2.225	≤±4%	30	Nadir	With 8 bits
<b>7</b>	2.235–2.285	≤±4%	30	Nadir	Signal Quantization
<b>8</b>	2.295–2.365	≤±4%	30	Nadir	
<b>9</b>	2.360–2.430	≤±4%	30	Nadir	

### **2.3 Summary**

This chapter presents the work of other researchers and the methods they applied in their different scopes of the study. These studies were reviewed and the important results from their works related to the study were mentioned. This chapter also consists the satellite image had been used in this research and also its characteristics.

## CHAPTER 3

### STUDY AREA, RESEARCH MATERIAL AND METHODOLOGY

#### 3.0 Introduction

This chapter describes the study area, research material and methodology related to this study. Basically, the properties and the characteristics of ALOS PALSAR and ALOS AVNIR-2 are presented and the image processing software involved to analyze the remote sensed data will be given. Subsequently, the processing steps involving all the datasets used in the study are addressed.

#### 3.1 Overview of Study Area

In this study, three study areas have been chosen which are located in northern peninsular Malaysia. These study areas include eastern part of Penang Island and Butterworth, northern part of Perak and southern part of Kedah are shown in Figure 3.1. These sites are selected because there are near to Universiti Sains Malaysia (USM) and for the purpose of carrying out ground truth.

##### 3.1.1 Penang

Penang is the second smallest and one of the thirteen states of Peninsular Malaysia. The study area is located in the eastern part of Penang Island and a portion of mainland called Butterworth. The geographical extent of the study area is between 578153.554mN and 612053.554mN and between 644065.806mE and 658690.806mE (Figure 3.1) which covers an area of approximately 510 km<sup>2</sup> (15 km x 34 km).

The ALOS PALSAR image (Figure 3.2) for Penang was acquired on 14 April 2009, and the ALOS AVNIR-2 imagery (Figure 3.3) on 15 December 2009. The satellite images for Penang were acquired at different dates. However, this would not bring any impact factor for land cover since both images were acquired in the same season. The seven classes identified for Penang are water, residential, urban, oil palm, paddy, bare land and forest.

While the island has an amazingly constant temperature, Penang's tropical location subjects to annual monsoons. The average temperature varies between 27 °C to 30°C throughout the year (NEA, 2012). The mean daily humidity varies between 60.9% and 96.8%. The two rainy seasons are southwest monsoons from April to October and north-east monsoons from October to February with annual rainfall averages 2670mm.

Penang Island is predominantly hilly terrain. The terrain encompasses coastal plains, hills and mountains (Ahmad et al., 2006). The population is mainly concentrated on the eastern side of the Island, probably due to the state capital (George Town) is situated and also its close proximity with the mainland. The topography Seberang Perai is relatively flat (Geography, 2012). It has a long coastline, the majority of which is lined with mangrove. Butterworth, the main town in Seberang Perai, lies along the Perai River estuary.



Figure 3.1 Location of the study area

### 3.1.2 Perak

The state of Perak is Peninsular Malaysia's second largest at 21,000 km<sup>2</sup> wide (Laporan Kiraan Permulaan, 2011), making up 6.4 percent of total land banks in Malaysia. The second study area is located in northern part of Perak. The area extends approximately from 534456.281mN to 581056.281mN and 649752.028mE to 668202.028mE, which covers an area of approximately 893 km<sup>2</sup> (19 km x 47 km) (Figure 3.1).

The ALOS PALSAR imagery (Figure 3.2) was acquired during the hot and dry season on 14 April 2009 and the ALOS AVNIR-2 image (Figure 3.3) was acquired on 30th July, 2009. The ALOS AVNIR-2 images were acquired during the rainy season. However, this difference in seasonality should not be an impacting factor, as most of the land covers/uses identified for this study site are not affected by seasonality.

The Perak's states climate is tropical monsoon, with offers bright sunny days and cool night's whole year through (Geography and climates of Perak, 2011). Temperature is fairly constant, varies from 23°C to 33°C, with humidity normally above than 82.3%. Annual rainfall measures at 3,218 mm.

The major urban developments in this region are around the city of Parit Buntar, seen in the top right corner of the images. With the exception of residential and urban areas in Parit Buntar, there are no other major cities in this study site. Majority of the flat valley is use for agricultural purposes include oil palm and paddy.



### **3.1.3 Kedah**

Kedah which sits up high in the northwest corner of Peninsular Malaysia is a fairly small state covering an area of 9,425 km<sup>2</sup> and its highest peak is Gunung Jerai, at 1200 meter above sea level. The final study area is located in southern part of Kedah, Malaysia (Figure 3.1). The area extends approximately from 593223.562mN to 639986.062mN and 662661.965mE to 677974.465mE, which covers an area of approximately 705 km<sup>2</sup> (15 km x 47 km).

The natural land cover was tropical broad-leaf rainforest. Now, forest remains only in the upland areas. The lowland areas are covered by rice paddy and other oil palm, field crops, roads, streams, bare land, and urban (Colbourne,2003).

Kedah enjoy a warm equatorial climate the whole year, with a uniform temperature between 21°C to 32°C throughout the year (Geography and climates of Kedah, 2011). From January to April, dry and warm weather with consistently high humidity on the lowlands averaging from 82 to 86 % per annum.

Kedah's average annual rainfall falls between 2,032 mm to 2540 mm with the wettest month from May to December. Kedah produces the most rice among the other states but the Government is attempting to diversify its economy, namely in industrial development (Geography and climates of Kedah, 2011).

### **3.2 Processing Software and Research Equipment**

Two main image processing software and research equipment have been applied in this research. ASF Map Ready 2.3 was used for pre-processing and PCI Geomatica 10.3.2 was applied for all image analyses related in this study. Garmin E-Trex Vista Hcx GPS was used for ground truth and validation of the results.

### **3.2.1 ASF MapReady 2.3**

The Alaska Satellite Facility develops and enhances software in order to simplify the use of Synthetic Aperture Radar (SAR) data. ASF MapReady 2.3 supports Single Look Complex (SLC) SAR data, ALOS optical data and quad-polarimetric SLC (i.e., ALOS PALSAR Level 1.1) data. It can be used for terrain correction, geocoding and converting SAR data from the original format to a GeoTIFF product which compatible with most of the image processing software. Polarimetric decompositions can be applied to multi-polarization SAR data. Other software included in the package is an image viewer, metadata viewer, and projection coordinate converter.

### **3.2.2 PCI Geomatica 10.3.2**

PCI Geomatica is a remote sensing desktop software package for processing earth observation data, designed by PCI Geomatics Inc. PCI Geomatica is aimed primarily at raster data processing and allows users to load satellite and aerial imagery where advanced analysis can be performed. All the processing such as geometric correction, mosaics, image enhancement, Ortho-rectification, speckle filter, texture analysis, computing math model and generated color-coded maps have been utilized using PCI Geomatica 10.3.2. PCI Geomatica has been used by many educational institutions and scientific programs throughout the world to analyze satellite imagery. With all the capabilities in this software, it definitely supports the needs of the study.